

Theoretical investigation of hydrogen storage in metal-intercalated graphitic materials

Manuel Cobian and Jorge Íñiguez

Institut de Ciència de Materials de Barcelona (ICMAB-CSIC), Campus UAB, 08193 Bellaterra, Spain

We have used first-principles methods to investigate how metal atoms dispersed in the interlayer space of graphitic materials affect their hydrogen-binding properties. We have considered ideal stage-one metal-intercalated graphites of various compositions as representative model systems. Our calculations suggest that alkaline earth metals can significantly enhance the hydrogen storage properties: for example, Be and Mg atoms would act as binding sites of three or four hydrogen molecules, with binding energies per H₂ in the 0.2–0.7 eV range, as required for applications. We also find that alkali and transition metals are not as effective in enhancing the storage capacity.

PACS numbers: 84.60.-h, 81.05.Uw, 71.20.Tx, 71.15.Pd

I. INTRODUCTION

Developing practical means to store hydrogen at ambient conditions is critical for the progress of fuel-cell technologies. The possibility of storing hydrogen in carbons attracts great interest, as they would constitute a light and cheap storage medium susceptible of large scale production. Unfortunately, the dominating carbon–hydrogen interactions that occur in the usual materials are not suitable for storage purposes: H₂ physisorption is too weak to retain the hydrogen at ambient conditions, and chemisorption of H atoms is too strong and hampers the hydrogen release.¹ Current efforts thus focus on obtaining binding interactions in the range that would be suitable for applications, namely, between 0.2 and 0.8 eV.

Recent *ab initio* simulations have suggested that carbon-supported transition^{2,3,4} and alkali⁵ metal atoms bind hydrogen with the appropriate interaction energy (e.g., about 0.5 eV per H₂ in Ti-decorated nanotubes) and are acceptable from a gravimetric viewpoint. Moreover, it seems that the predicted binding mechanism has been observed experimentally in multiwalled nanotubes on which nickel nanoparticles were dispersed.^{6,7} Those promising results clearly indicate this storage strategy deserves further study. However, it is also evident that the new metal-mediated hydrogen-storage mechanisms will be useful only if they are present in materials that are easy to produce (e.g., the usual activated carbons or graphitic nanofibers) and free from problems that could impede a practical application (e.g., oxidation or segregation⁵ of the metal atoms). So far, the simulations have focused on cases in which the metal atoms are deposited on free-standing nanotubes or fullerenes. Such model systems may be expected to mimic the situation in the walls of the large pores present in many carbons. Unfortunately, the calculations indicate that, except for the case of Li, such materials are bound to suffer from metal segregation and clustering problems.

A possible strategy to diminish the segregation problem is to look for materials in which the metal atoms are more tightly bound to the carbon structure. That should be the case of metal-intercalated graphites, graphitic nano-fibers, and carbons of the type used for electrodes

in lithium batteries. Continuous progress in the synthesis of intercalated graphites (which is best illustrated by the recent obtention^{8,9} of massive samples of stage-one crystalline C₆Ca) and carbons for battery electrodes provides encouragement for a theoretical investigation of such possibilities, as it suggests that predictions of new materials may be experimentally realizable.

We have thus studied this general class of materials, in which the metal atoms can appear *sandwiched* between graphene layers, using first-principles simulation methods. Since this work aims at identifying trends as a function of the metal species and quantifying the dominant interactions involving hydrogen, we have focused on the simplest model systems capturing the relevant chemical and physical effects: *stage-one* metal-intercalated graphites of various compositions. (The term *stage-one* implies that all the interlayer spaces have the same metal content.) Note that, strictly speaking, some of the graphites considered might be impossible to obtain experimentally because of staging effects¹⁰ that we do not intend to address here. Yet, the phenomena occurring in the vicinity of the metal atoms in our simulated systems can be expected to occur also in the other carbons mentioned above.

The paper is organized as follows. Section II describes the employed methodology, with special emphasis on the status of Density Functional Theory^{11,12} (DFT) methods regarding van der Waals interactions and the practical approach adopted here. In Section III we present and discuss our results for alkali (Subsection A), alkaline earth (Subsection B), and representative transition (Subsection C) metals. In Subsection D we discuss results pertaining to the binding of the metal atoms to the carbon structure and the possibility that segregation occurs. Finally, in Section IV we give our summary and conclusions.

II. METHODOLOGY

We used the Local Density (LDA) and Generalized Gradient (GGA) Approximations to Density Functional Theory as implemented in the code VASP.¹³ More pre-

cisely, we used the Perdew-Zunger parametrization¹⁴ of Ceperley-Adler data¹⁵ for the LDA, and the so-called GGA-PBE of Ref. 16. The PAW scheme^{17,18} was employed to represent the atomic cores. Nominal valence electrons were explicitly treated, as well as the semi-core electrons of all the metal atoms considered (e.g., the $3s$ and $3p$ electrons of Sc). We used a plane-wave basis with a 400 eV cut-off, and k-point grids with spacings that were in all cases smaller than 0.07 \AA^{-1} ; we checked these calculation conditions lead to sufficiently converged results. We also used the first-principles software package PWscf¹⁹ to analyze the electronic properties of the most relevant structures obtained with VASP. We found spin polarization only in a few of the systems considered (the metal-doped single graphene layers and the graphites intercalated with nd^3 transition metals). Thus, the vast majority of the studied materials, including the most relevant ones for hydrogen storage purposes, contain no unpaired electrons.

The van der Waals interactions, responsible for the physisorption of H_2 in carbons, are likely to play an important role in many of the systems considered here. The status of DFT in relation to van der Waals forces is an awkward one: while it is known that the usual LDA and GGA's are ill-suited to model such interactions, for many physisorption systems the LDA renders binding energies that are (albeit accidentally) in reasonable quantitative agreement with the experiment.²⁰ (The GGA, on the other hand, usually renders significantly smaller or even repulsive interactions.^{21,22}) More specifically, Ferrel-Vilaplana²³ has performed careful (and computationally costly) MP2 studies correcting for basis-set superposition errors, and found that the binding energy of H_2 physisorbed on graphene is about 0.064 eV, to be compared with the LDA result of 0.083 eV.²⁰ While this result clearly indicates a serious overbinding associated to the LDA, it also suggests the LDA binding energies can be considered as qualitatively correct, with a *systematic* quantitative error of about 30%. Having this in mind, many authors have regarded LDA as a reasonably reliable and computationally efficient method to study this type of systems. Here we adopt the same approach. Finally, note that for some of the materials studied – most importantly, for the graphites intercalated with alkaline-earth metals –, we found that the dominant interactions are not of a dispersive nature. In such cases, in which DFT can be expected to be quantitatively accurate, we performed GGA calculations to ratify the LDA results.

It should also be noted that in our simulations we did not consider the quantum mechanical nature (i.e., quantum-rotor effects) of the hydrogen molecules. Such a simplified representation becomes accurate whenever the molecules are tightly bound or the interactions are as large as to cause H_2 dissociation. For all other cases, the approximation of treating the hydrogen molecules as classical objects must be born in mind. Note also that we did not consider thermal effects in the calculations and, thus, all the obtained results correspond to the zero

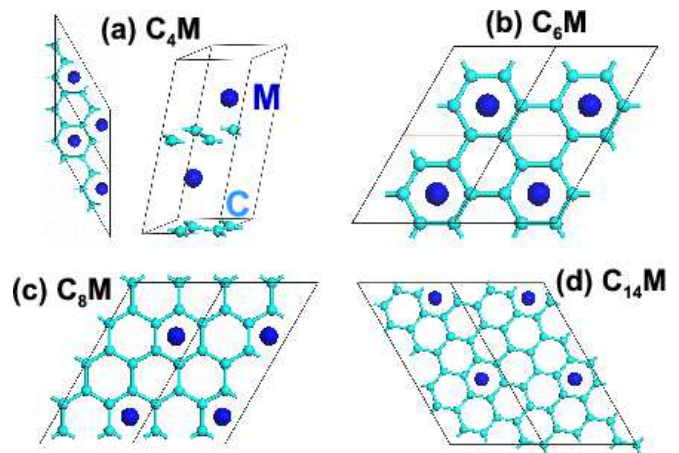


FIG. 1: (Color online) Schematic representation of the four basic model systems considered in this study. A top view of a 2×2 in-plane repetition of the supercell is shown in all the cases; for the C_4M composition in panel (a), a lateral view of the supercell is also shown.

temperature limit and directly reflect the fundamental interactions.

Our simulations were aimed at the computation of the binding energy between hydrogen molecules and various metal-intercalated graphites. Binding energies (E_b 's) are computed as the energy difference between the bound system and its constituents. For example, the binding energy of H_2 to the C_4Li intercalated carbon is given by $E(\text{H}_2) + E(\text{C}_4\text{Li}) - E(\text{C}_4\text{Li-H}_2)$, where $E(\text{H}_2)$ is the energy of the isolated hydrogen molecule relaxed to its equilibrium (lowest-energy) configuration, etc. The H_2 molecules were introduced in the system one at a time, which allowed us to compute the binding energy as a function of hydrogen load.

Figure 1 represents the main model supercells considered, which correspond, respectively, to the chemical formulas C_4M , C_6M , C_8M , and C_{14}M , where M is the metal atom. Note that, as shown in panel (a) for the C_4M case, our supercells included two graphene layers (and, thus, two interlayer spaces with metal atoms) whose relative position was allowed to evolve freely towards the lowest-energy solution during the structural relaxation. Given the intricate energy landscape associated to the materials considered, we found it necessary to perform the structural relaxations in a very meticulous way: We first ran a short (50 fs) constant-energy molecular dynamics with initial random velocities corresponding to a temperature in the 100-700 K range; the obtained structure was then used as the starting point of a full relaxation of atomic positions and cell parameters. The structural relaxations were regarded as completed when residual forces (stresses) were smaller than 0.05 eV/\AA (0.05 GPa); we checked this criterion leads to sufficiently accurate energies. For all the systems considered, the described procedure was repeated a minimum of 7 times (up to a maximum of 40 times in specially difficult or significant

cases) starting from different initial configurations, from which only the lowest-energy solution was taken into account for further considerations. (We wanted to study the behavior of these materials at room and higher temperatures; thus, restricting ourselves to the lowest-energy solutions seemed perfectly justified.) The initial configurations were carefully chosen so as to cover a range of possibilities as broad as possible; in particular, for all the compositions studied, we considered initial configurations involving molecular and atomic hydrogen, so as to be able to determine in which cases H_2 dissociation is energetically favorable. We explicitly checked this relaxation scheme leads to the correct result in *simple* cases with only one H_2 molecule *per* metal atom, for which it is possible to identify the global minimum by starting relaxations from all possible critical points (i.e., maxima, minima and saddle points) of the complex energy landscape of the system.

It is worth to comment on the possible errors associated to our particular choice of model systems and relaxation scheme. The size of the considered supercells determines the number of independent atoms in our simulations, defining the configuration space explored in the structural relaxations. Having relatively small supercells may thus be problematic, specially in cases in which H_2 molecules dissociate and form metal-hydrogen complexes. Being aware of this, we checked the suitability of the smallest supercell considered (shown in Fig. 1a) by repeating the study of some compositions using a supercell twice as big (doubled in the plane). We did not find any qualitative changes with respect to the results obtained with the small supercell, which suggests we can trust the qualitative correctness of our results. At any rate, it is important to realize that these finite-size errors, as well as other possible errors in the identification of the global minima, inevitably become worse as the number of H_2 molecules increases, implying that our calculated hydrogen-binding energies will be smaller than the ones we would *ideally* obtain. Hence, errors of this nature are actually quite benign, as they result in an underestimation of the H_2 -storing ability of these materials.

III. RESULTS AND DISCUSSION

We find that the electronic structure of the metal atom completely determines the system's hydrogen-storage properties. Accordingly, we have divided our results in three groups, which correspond to the alkali, the alkaline earth, and the transition metals, respectively.

A. Alkali metals

1. Simulation results

Table I summarizes our results for the binding energies and Fig. 2 shows the lowest-energy configuration of

TABLE I: Calculated binding energies (in eV) of hydrogen molecules absorbed in stage-one graphites intercalated with alkali metal atoms. We considered the insertion of H_2 molecules in the system one at a time, so as to compute the dependence of the binding energy with the hydrogen load. For example, the result for C_6Li-nH_2 and $n=2$ is obtained from $E(C_6Li-H_2) + E(H_2) - E(C_6Li-2H_2)$. For each system, we show results up to the maximum number of H_2 molecules per metal atom that can be absorbed (n_{\max}), which varies with the carbon-metal ratio. The average binding energy per molecule (\bar{E}_b) is obtained from the fully hydrogen-loaded result as $[E(C_6Li) + n_{\max} E(H_2) - E(C_6Li-n_{\max}H_2)]/n_{\max}$. We also indicate the hydrogen weight percentage corresponding to $n=n_{\max}$.

System	n=1	n=2	n=3	... n=6	\bar{E}_b	wt.%
C_6Li-nH_2	-0.23	0.18			-0.03	4.9
C_8Li-nH_2	-0.14	0.16	0.31		0.11	5.6
$C_{14}Li-nH_2$	-0.27	0.23	0.22	0.23	0.14	6.5
C_6Na-nH_2	0.31	0.30			0.30	4.1
C_8Na-nH_2	0.29	0.32	0.31		0.31	4.8
$C_{14}Na-nH_2$	0.24	0.29	0.33	0.26	0.27	6.0
C_6K-nH_2	0.32	0.24			0.28	3.5
C_8K-nH_2	0.32	0.34	0.17		0.28	4.3
$C_{14}K-nH_2$	0.28	0.38	0.28	0.21	0.26	5.5

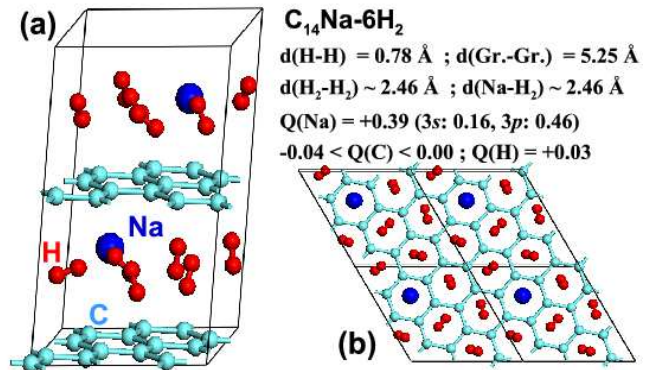


FIG. 2: (Color online) Lateral (a) and top (b) views of the lowest-energy configuration computed for the $C_{14}Na-6H_2$ composition. In panel (b) a 2×2 in-plane repetition of the considered supercell is shown. The relevant distances and Löwdin charges (in elementary charge units) are given. The in-plane lattice parameters are essentially unaffected by the insertion of metal and hydrogen atoms.

$C_{14}Na-6H_2$, which is a representative case. In the Na compounds, we find that the binding energy of all the absorbed molecules is about 0.3 eV and is largely independent of the amount of hydrogen present. The situation is similar for K, although the dependence of E_b with the amount of stored hydrogen is more significant. In the case of Li, on the other hand, the binding energy of the first H_2 molecule is negative, implying that the absorption is not energetically favorable. However, the

absorption of additional molecules is predicted to occur, with binding energies of as much as 0.3 eV. (This seemingly puzzling behavior is explained in the *Interpretation* section below.) Finally, the metal content seems to have a relatively small influence in the binding properties, as we observe no drastic effect associated to the C–M ratio.

The obtained lowest-energy solutions are, without exception, characterized by the following two features: (1) The graphene layers are perfectly superimposed in an *eclipsed* configuration (i.e. an “AA stacking”). (2) The hydrogen molecules position themselves in the space between two eclipsed carbon hexagons, and tend to align with the direction perpendicular to the graphenes. The observed deviations from an homogeneous alignment of the H₂ molecules are probably the reflection of a complex multi-minima energy landscape, determined by small H₂–H₂ and H₂–carbon/metal interactions whose magnitude falls below the accuracy requested in our structural relaxations. As indicated in the previous Section, we explicitly considered the possibility of H₂ dissociation by choosing appropriate initial configurations for the structural relaxations (i.e. configurations in which we start with two separated H atoms instead of an H₂ molecule). However, from such calculations we always obtained either a higher-energy solution or a recombination of the H atoms to form a molecule. Moreover, we never observed H₂ dissociation in relaxations where the starting point was molecular hydrogen.

In what regards the electronic structure of the lowest-energy configurations, a standard analysis in terms of Löwdin charges²⁴ indicates that the cation donates most of its valence electron to the graphene layers, which are thus negatively charged. Interestingly, the charges computed for the metal and carbon atoms remain essentially unaffected by the insertion of H₂ molecules; accordingly, the molecules do not charge significantly, and an analysis of the electronic wave functions indicates very weak bonding with the carbon or metal atoms. (Such weak bonds are typical of LDA simulations of van der Waals systems. While known to be an artifact of the theory, they render an interaction of a magnitude that is similar to that of the actual van der Waals forces, as mentioned in Section II.) The calculated H–H distances are always around 0.78 Å, closely resembling the 0.77 Å that the LDA renders as the equilibrium bond distance of an isolated H₂ molecule.

2. Interpretation

To understand these results, it is useful to consider the absorption of molecular hydrogen in graphite when no metal atoms are present. In that case, our LDA scheme predicts a binding energy of 0.13 eV per molecule in the fully-loaded situation corresponding to a CH chemical formula. (We denote as “fully loaded” the case in which there is one H₂ molecule in every *site* between C₆ hexagons.) On the other hand, when only a

few H₂ molecules are inserted into the structure, the graphite–H₂ interaction turns out to be repulsive (we computed a negative binding energy of –0.07 eV per molecule for the C₈H₂ system). These results, which agree with earlier theoretical studies,²⁵ reflect the competition of interactions that is at play in the hydrogen sorption process. In essence, the insertion of hydrogen causes an increment of the graphene–graphene interlayer distance, which switches from the 3.4 Å computed for pure graphite to the 5.2 Å obtained for the fully hydrogen-loaded material. The absorption of only a few H₂ molecules is thus energetically unfavorable, as the energy gain associated to the graphene–H₂ interaction cannot compensate for the energy cost associated to the increased interlayer distance. (Roughly, our results indicate that the interlayer binding energy in graphite is about 0.02 eV per C atom, and that the graphene–H₂ interaction energy *within graphite* is about 0.11 eV.) As more hydrogen goes into the system, by applying H₂ pressure experimentally, the energy balance switches sign and we obtain a net binding energy per H₂ molecule.

In our alkali metal-intercalated graphites, the interlayer distances in the systems without hydrogen are 3.4, 4.3, and 4.9 Å, respectively, for Li, Na, and K (the values correspond to the materials with C₁₂M chemical formula and are representative for the rest). Thus, it is not surprising that the materials with Na and K can uptake H₂ molecules, since the interlayer distance is nearly unaffected by the hydrogen absorption and, thus, there is no energy cost associated to an interlayer expansion. The case of Li, on the other hand, is very similar to that of metal-free graphite, i.e., the absorption is favorable only when a large enough number of hydrogen molecules are involved. This picture is essentially identical to the one proposed to explain early experimental results for the absorption of hydrogen and larger molecules in K-intercalated graphites.²⁶

The above reasoning suggests it might be possible to store hydrogen molecules at binding sites that do not have any neighboring metal atom, provided that the interlayer distance is large enough. We thus considered systems of composition C₁₈M–nH₂, in which binding sites isolated from the metal atoms exist, and performed the kind of study described above. In the case of Na, the computed binding energy was 0.27 eV for H₂ molecules neighboring a metal atom, and 0.23 eV for those that do not have any metal as first neighbor. We obtained the same qualitative results for the Li (0.13 eV average E_b for molecules neighboring a metal atom and 0.19 eV for the additional ones) and K (with binding energies of 0.26 eV and 0.22 eV, respectively) systems. These results strongly support the notion that the enhancement of the H₂ binding is related to the increase of the interlayer distance caused by the metal atoms, and not to a direct metal–H₂ coupling. It is worth to mention here that this conclusion contrasts with theoretical studies of Li-doped graphene: in that case, an *enhanced-physisorption* type of interaction was found for H₂ molecules in the vicinity

of the alkali metal atom, the enhancement being associated to a significant charge transfer to hydrogen.²⁷ In addition, electrostatic interactions between free-standing alkali metal atoms and H_2 molecules,²⁸ associated to quadrupoles and induced dipoles, are known to exist, and one might have expected them to play a role in the systems here considered. However, our results indicate that such charge transfer and electrostatic effects are secondary for the hydrogen interactions in graphites intercalated with alkali metals.

We performed a second computer experiment aimed at ratifying the above conclusions. We considered the system that can be described as the periodic repetition of the $\text{C}_6\text{-Na-C}_6\text{-}$ motif, in which half of the interlayer spaces are free from metal atoms. (This would correspond to a *stage-two* intercalation.) In this case, we obtained an average binding energy of 0.11 eV for the molecules in the metal-free interlayer space, which is very close to the value reported above for the absorption of H_2 in pure graphite. This result confirms that it is the expanded interlayer distance, and not the fact that the graphene layers are charged, what facilitates the binding of H_2 molecules in these systems.

3. Discussion and connection with experiment

Our simulations indicate that alkali metals intercalated in graphite enhance the binding properties of the system, and that the effect holds for a wide range of carbon-metal ratios. We find that the metal atom plays the role of increasing the interlayer distance, thus allowing a more energetically favorable absorption. As mentioned above, such a conclusion is essentially in agreement with what was experimentally observed²⁶ in studies of the absorption properties of K-intercalated graphites.

The experimental work on state-two C_{24}K offers some quantitative data that can be used to check the soundness of our simulations. Most significantly, it is observed experimentally that, upon absorption of H_2 , the inter-graphene distance expands by about 0.29 Å.²⁶ This is compatible with our results for stage-one C_{14}K , the closest composition we have studied, for which we observe that the addition of two H_2 molecules per metal atom shifts the interlayer spacing from 4.90 Å to 5.17 Å. The measured heat of absorption, on the other hand, is about 2.3 kcal/mol (i.e., 0.10 eV per H_2 molecule).^{26,29} Such a quantity is not directly comparable to the binding energies of about 0.28 eV per H_2 that we obtained for the compounds with K, since we did not include thermal effects in the calculations. Yet, other authors²⁹ have obtained a remarkable agreement with the experimental heat of absorption from molecular dynamics simulations that were based on a first-principles approach essentially identical to the one used here. Thus, we can conclude our calculations are reliable, at least at a qualitative level, for the prediction of the absorption energetics.

A critical discrepancy between the experiment and our

theory pertains to the number of H_2 molecules per metal atom that can be absorbed by the system. For stage-two C_{24}K , the experiments clearly indicate a maximum uptake of two hydrogen molecules per metal.^{30,31} Moreover, it is found that stage-one C_8K , one of the systems we have simulated, does not absorb any hydrogen unless significant pressures are applied: 100 atms are necessary to obtain $\text{C}_8\text{K-2H}_2$.³² It is thus obvious that a *naïve* theoretical prediction for large storage capacities, as suggested by the binding energies in Table I, is not realized experimentally. Several causes might be at the origin of this conflict. First of all, one should not forget that the underlying LDA approximation is surely overestimating the H_2 binding energies at large hydrogen contents, and might also fail to properly describe the $\text{H}_2\text{-H}_2$ repulsion at short distances. In addition, it should be noted that our theoretical representation of the physisorbed H_2 does not reflect the actual *effective size* of the molecule, which is determined by the quantum nature of hydrogen as well as by thermal effects. Indeed, in the discussion given in Ref. 26, the effective diameter of H_2 is taken to be of about 2.4 Å; when the effective size of the metal ions is also considered, one quickly runs into steric restrictions for the absorption of hydrogen into the system. In particular, it is found that there is not sufficient space for any hydrogen molecule in the C_8K structure or for a third molecule, per metal atom, in the C_{24}K compound. In consequence, one has to be cautious when drawing conclusions from our simulations of hydrogen-loaded graphites, which are characterized by very densely packed molecules. (Note that, in the fully hydrogen-loaded lowest-energy structures, the average $\text{H}_2\text{-H}_2$ distance coincides with the distance between hexagon centers in graphene, which is about 2.46 Å.) Indeed, a full statistical and quantum-mechanical study would be necessary to determine the actual significance of the lowest-energy structures found. In principle, two scenarios are possible: such structures might turn out to be either (i) metastable configurations that would be accessible upon overcoming an energy barrier, or (ii) unstable configurations that can be realized only by the continued application of high hydrogen pressures. Given the relatively small binding energies per molecule that we obtained, the second possibility seems more likely.

In conclusion, our results for graphites intercalated with alkali metals are essentially in agreement with what was known about such systems. Thus, they have not revealed any novel physical or chemical effect that might have an impact in hydrogen-storage applications.

B. Alkaline earth metals

1. Simulation results

Most importantly, and at variance from what we obtained for the alkali metals, in this case we find that the H_2 molecules react chemically with the metal atom. The

TABLE II: Calculated binding energies (in eV) of hydrogen molecules absorbed in stage-one graphites intercalated with alkaline earth metal atoms. The information is organized as in Table I. The values between parenthesis correspond to situations in which the H_2 molecules are physisorbed (see text). In the “ \bar{E}_b ” and “wt.%” columns, the values between parenthesis are computed including the physisorption cases.

System	n=1	n=2	n=3	n=4	\bar{E}_b	wt.%
C_4Be-nH_2	0.76	0.50	(0.15)	(0.17)	0.63 (0.39)	6.6 (12.4)
C_6Be-nH_2	0.29	0.70	0.52	(0.05)	0.50 (0.39)	7.0 (9.1)
C_4Mg-nH_2	0.73	0.50	0.36	(0.08)	0.53 (0.41)	7.7 (10.0)
C_6Mg-nH_2	0.24	0.25	0.16	0.24	0.22	7.7
C_4Ca-nH_2	0.43	-0.15	0.24	0.02	0.14	8.4
C_6Ca-nH_2	0.41	-0.24	0.34	-0.02	0.12	6.7

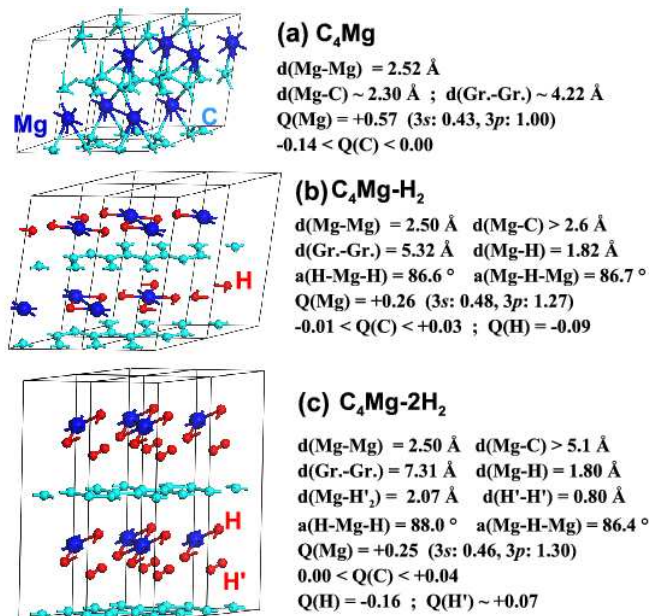


FIG. 3: (Color online) Lateral view of the lowest-energy configurations obtained for the C_4Mg (a), C_4Mg-H_2 (b), and C_4Mg-2H_2 (c) compositions. A $2 \times 2 \times 1$ repetition of the considered supercell is shown. The relevant distances, angles and Löwdin charges (in elementary charge units) are given. The in-plane lattice parameters are essentially unaffected by the insertion of metal and hydrogen atoms.

computed binding energies are given in Table II. The most interesting results correspond to the materials with Be and Mg, which present a similar phenomenology and can be described jointly.

Figure 3 displays the results for the C_4Mg-nH_2 systems, which are representative of the rest. (Note that the metal density of the C_4M systems is so high that the metal atoms fall within bonding distance of each other.) As shown in Fig. 3(a), the Be/Mg atoms do not place themselves at the central point between two eclipsed C_6 hexagons, but adopt a less symmetric and less coordi-

nated configuration. Figure 3(b) shows the lowest-energy solution resulting from the absorption of a first H_2 . We found that, in all the cases considered, this first hydrogen molecule dissociates and the individual H atoms form chemical bonds with the metal. The results for the second H_2 molecule are illustrated in Fig. 3(c): it places itself in the neighbourhood of the metal atom and undergoes a considerable elongation, the H–H bond distance increasing up to typical values between 0.80 and 0.83 \AA . The behavior of additional H_2 molecules varies from system to system, in a way that seems to be strongly correlated with how much room there is available in the neighbourhood of the metal atom. For example, in the case of C_6Be-3H_2 the third molecule binds to the Be atom in the same way as the second one; in contrast, in the more densely-packed C_4Be-3H_2 system the third hydrogen cannot access the metal and *physisorbs* into the structure, the computed H–H distance being 0.77 \AA (the corresponding binding energy is given between parenthesis in Table II). In both the Be and Mg cases, we found it impossible to insert a fifth H_2 into the system.

The behavior of the Ca compounds is more complex. As in the cases of Be and Mg, the first hydrogen molecule dissociates, and the individual hydrogens form bonds with the metal. However, we found that the addition of a second H_2 is not energetically favorable. Moreover, the lowest-energy configuration is one in which there is no dissociated hydrogen molecule. Instead, the two molecules per metal are bound to the Ca atom and significantly elongated, the typical H–H distance being 0.86 \AA . It is noteworthy how the dependence of the interlayer distance with the hydrogen content reflects these binding trends; for the C_6Ca-nH_2 systems we obtained: 4.51 \AA for $n=0$ (i.e. the system without hydrogen), 5.09 \AA for $n=1$, and 4.66 \AA for $n=2$. The relatively large interlayer spacing for the $n=1$ case reflects the strong Ca–H interaction and the concomitant weakening of the C–Ca bonds. When, for $n=2$, we switch to a weaker Ca– H_2 interaction, the interlayer distance reduces to a value that is close to that of the $n=0$ case. Interestingly, the addition of a third H_2 molecule is energetically favorable and, in this case, the lowest-energy solution displays two molecules weakly bound to the metal atom, with a typical H–H distance of 0.80 \AA , and two individual hydrogen atoms that form chemical bonds with Ca. The interlayer distance for $n=3$ is computed to be 6.91 \AA , which again reflects that the C–Ca interactions are weakened by the formation of Ca–H bonds. A fourth H_2 remains molecular and its net interaction with the rest of the system is negligible.

Also given in Figure 3 are the Löwdin charges computed for the C_4Mg-nH_2 systems. They display the following features that are, in essence, common to all the systems studied: (1) In the materials without hydrogen, there is a significant charge transfer from the metal to the graphene layers; also, the empty p orbitals of the metal get populated and play an important role in the C–M bonds. (2) The dissociation of H_2 is related to a con-

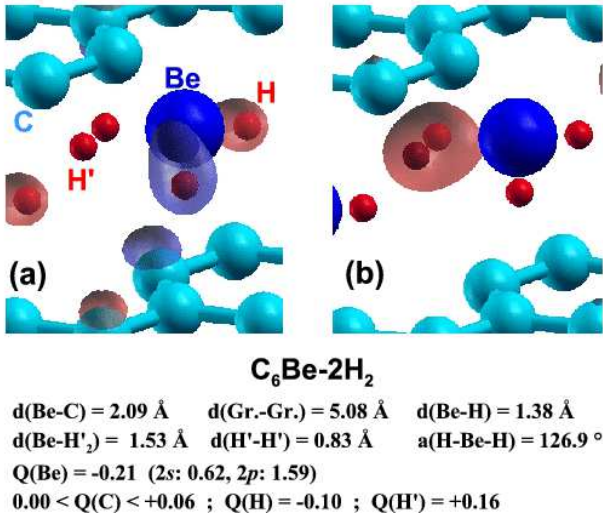


FIG. 4: (Color online) Computed metal–hydrogen binding eigenstates of the C₆Be-2H₂ system, corresponding to the Γ -point of the Brillouin zone.³³ Panel (a): Highest occupied electronic state, which is associated to the bonding between Be and the individual H atoms. The character of the wave function is predominantly H-1s and Be-2p, as evidenced by the different sign (different color in the figure) of the lobes stretching from the metal to the hydrogens. Panel (b): Low-lying electronic state with predominant H-1s character. In essence, this is the bonding σ -orbital of the H₂ molecule, which is only partly occupied as charge is transferred to Be-2p orbitals. The relevant distances, angles, and Löwdin charges (in elementary charge units) for the C₆Be-2H₂ system are given.

siderable charge transfer from the metal to the hydrogen atoms. As illustrated in Fig. 4(a) for the case of C₆Be-2H₂, the individual H atoms form bonds with the metal and are negatively charged by about 0.10 electrons. (3) The interaction between the metal atoms and the elongated H₂ molecules involves a charge transfer that has a marked one-directional character: the empty *p* orbitals of the metal drag about 0.1-0.2 electrons from the binding σ -orbital of the molecule (a typical low-lying M–H₂ binding state is displayed in Fig. 4(b)). The calculations clearly show there is no charge back-donation from the metal to the anti-bonding σ^* -orbital of the hydrogen molecule. (4) As the hydrogen content increases, the graphene layers tend to donate charge to the metal–hydrogen complex.

Since our simulations predict chemical reactions and bond formation in the case of the alkaline earth metals, it seems mandatory to ratify the LDA results of Table II with GGA simulations, which are well-known to be more accurate in this context.¹⁶ Hence, we performed GGA calculations for the C₄M-nH₂ systems with M = Be and Mg. In the Be case, we obtained binding energies of 0.62 eV for n=1 and 0.31 eV for n=2; these results imply a 0.1-0.2 eV correction (reduction) of the values in Table II. On the other hand, for the physisorbed molecules corresponding to n=3 and n=4, the GGA renders re-

pulsive/negligible interactions of -0.12 and 0.00 eV, respectively. In the Mg case, the GGA binding energies for n=1, 2, and 3 are, respectively, 0.55, 0.41, and 0.03 eV. The only significant deviation from the results in Table II pertains to the third H₂ molecule, whose LDA binding energy is 0.36 eV. Such a discrepancy probably reflects the complex nature of the binding interactions associated to that hydrogen, which might be a combination of chemical bonding to the metal and physisorption to the carbon structure. Finally, the GGA binding energy for the fourth molecule, which is undoubtedly physisorbed, is negative: -0.07 eV. In conclusion, our selected GGA calculations ratify the conclusions drawn from the LDA simulations, and indicate an LDA overestimation of about 0.1 eV for the energies associated to chemical bonds.

2. Discussion

We have thus found that the intercalation of alkaline earth metals results in hydrogen-binding properties that differ significantly from those obtained by intercalating alkali metals. The alkaline earth metals considered react chemically with the hydrogen molecules, which results in either (i) the dissociation of the molecule to form M–H bonds, or (ii) the formation of a M–H₂ bond via a mechanism that involves a significant charge transfer from the hydrogen molecule to the metal. Interestingly, this difference in behavior between the elements of the first two columns of the Periodic Table had already been pointed out in the literature. For example, Ref. 28 reports a theoretical study of the interactions of H₂ with a number of free-standing ions (e.g. Li⁺, Na⁺, and Mg²⁺) and concludes that charge donation from the σ orbital of hydrogen to the low-lying empty orbitals of the metal does occur for Mg²⁺ but not for the alkali metals; such an observation is consistent with our results. In addition, the authors of Ref. 28 did not observe any back-donation from the filled metal orbitals to the anti-bonding σ^* -orbital of the hydrogen molecule, again in accordance with our findings and in contrast with what is typical in transition-metal–H₂ Kubas complexes.³⁴

Our results thus suggest that inserting alkaline earth metal atoms in graphite-like structures should result in a significant enhancement of the hydrogen sorption and storage properties. One might question the reliability of this prediction, as in the case of the alkali metals everything indicates that LDA-related errors, as well as neglected quantum and thermal effects, add up to cause a large discrepancy between the predicted hydrogen-storage capacity and the observations for K-intercalated graphites. The situation seems qualitatively different for the alkaline earths, though. First of all, in this case the hydrogen absorption relies on the formation of chemical bonds with the metal atoms, a situation for which DFT is known to be reasonably accurate. Secondly, the presence of those chemical bonds suggests that, at variance with what is assumed for the H₂ molecules physisorbed

within the alkali-intercalated graphites,²⁶ here it does not make sense to associate a large effective diameter to the absorbed hydrogen molecules. This is further supported by the results of vibrational calculations, restricted to the hydrogen atoms, that we performed for representative cases: For C_6Mg-2H_2 the lowest-lying frequencies computed are about 270 cm^{-1} , reflecting relatively strong metal–hydrogen interactions, while for $C_{14}Na-6H_2$ and $C_{14}K-6H_2$ we obtained modes with frequencies as low as 150 cm^{-1} , indicating that the hydrogen molecules are not bound as strongly. For these reasons, we believe the theoretical storage-capacity values reported in Table II for the alkaline earths can be taken as relevant for the actual materials.

In summary, we can conclude that the intercalation of alkaline earth metal atoms in graphitic carbons may result in useful materials for hydrogen storage. It would thus be interesting to study the sorption of hydrogen by, for example, the recently obtained stage-one C_6Ca intercalated graphites.^{8,9} We hope our work will also stimulate efforts to produce similar intercalated graphites using Mg and Be, or to investigate carbons of the type used as electrodes in Li batteries, but intercalated with alkaline earth metals rather than with lithium.

C. Transition metals: results and discussion

We only studied in detail a few transition metals (Sc, Ti, V, Y, and Zr), which was sufficient to identify general trends. Our main findings are summarized in the following points. (All the numerical results correspond to C_6M-nH_2 compositions.) (1) The first H_2 molecule interacts with the metal atom, drawing charge from it, and dissociates. The associated binding energy increases strongly as we move down and to the left in the Periodic Table. More precisely, we obtained positive bindings for Sc (0.08 eV), Y (1.11 eV), and Zr (0.23 eV), and repulsive interactions of for Ti (−0.30 eV) and V (−1.04 eV). (2) We tried the addition of a second H_2 molecule in the Sc, Y, and Zr compounds. The absorption was found to be energetically favorable only in the Sc compound, with a small associated binding energy of 0.03 eV. The strongest repulsion corresponds to the material with Y (−0.47 eV). In all the cases considered, the second H_2 was found to remain molecular and bind to the metal atom, the typical H–H bond distance obtained being about 0.86 Å. The resulting metal–hydrogen complexes have the form $M-2H-H_2$, as we did not observe any recombination of the H atoms coming from the dissociation of the first hydrogen molecule. Given that these results are not encouraging from the hydrogen-storage perspective, as it is clear that the only hopes (if any) are associated to relatively heavy elements, we did not consider the insertion of a third H_2 molecule.

The results for the first H_2 molecule can be understood by noting the strong correlation between the computed binding energies and the graphene–graphene interlayer

distances in the materials without hydrogen. Indeed, the hydrogen-free systems display very compact C_6-M-C_6 structures and strikingly short interlayer distances. More precisely, for the $3d$ metals considered, i.e. Sc, Ti, and V, we obtained 3.82, 3.50, and 3.26 Å, respectively; for the $4d$ metals, Y and Zr, we got 4.30 and 4.03 Å, respectively. (Keep in mind that our LDA equilibrium interlayer distance for graphite is about 3.4 Å.) The insertion of H_2 causes an expansion of the interlayer space and, naturally, such an expansion will be greater, and energetically more costly, in the materials presenting smaller interlayer distances in the hydrogen-free case. Indeed, we obtained that the insertion of H_2 is most energetically unfavorable in the Ti and V compounds, where the graphene–graphene distance grows up to 4.29 and 3.98 Å, respectively, upon the absorption of H_2 . In contrast, it is comparatively easy for the H_2 molecules to enter the interlayer space in the Y compound (the interlayer distance obtained in the C_6Y-H_2 case is 4.83 Å).

In what regards the second H_2 molecule, the situation becomes more complicated. Most noticeably, the Y compound, which is the material in which more interlayer space is available, is also the one displaying a stronger repulsion. Such a result can probably be attributed to the existence of very stable $C_6-(Zr-2H)-C_6$ groups that do not gain any energy by binding an additional H_2 .

From our Löwdin analysis, we did not observe any remarkable feature concerning the C–M interactions leading to the very short interlayer distances mentioned above. The C–M bonding seems very similar to that occurring between transition-metal atoms and carbon nanotubes or fullerenes, which has already been discussed in the literature (see Ref. 4 and references therein). One could nevertheless be suspicious about the LDA for this type of calculation, since this approximation is known to overestimate the strength of chemical bonds, which might be resulting in unrealistically small interlayer distances. Hence, for a number of representative cases we repeated our calculations using the GGA. For example, for the hydrogen-free graphites with Sc, Ti, and Y, the GGA renders, respectively, the following interlayer distances: 3.89, 3.58, and 4.41 Å. For the same systems, the GGA binding energy for the first H_2 molecule is, respectively, −0.18, −0.91, and 0.82 eV. Thus, as we found in the case of the alkaline earth metals, the GGA corrects the overbinding associated to the LDA, and can even switch the sign of the interaction in cases where the LDA predicts very weak binding (e.g. in C_6Sc-H_2). Yet, generally speaking, the GGA corrections are not qualitatively significant and our LDA-based conclusions remain valid.

Consequently, none of the transition metals considered appears as a good option to enhance the hydrogen-storage capacity of graphitic materials. Our simulations predict strong carbon–metal interactions that preclude the possibility that the metal atoms act as convenient binding sites for hydrogen.

D. Stability of the metal-intercalated systems

Finally, we report results concerning one of the basic motivations to study this class of materials: the notion that graphitic systems may bind individual metal atoms tightly enough to preclude metal-segregation and clustering problems that would complicate hydrogen-storage applications.

In principle, to investigate the segregation of metal atoms in these materials one would need to perform molecular dynamics simulations that capture the thermally activated diffusion mechanisms. Unfortunately, that constitutes a very computationally demanding work that falls beyond the scope of the present study. Nevertheless, one can try to quantify the tendency to cluster of the different elements by comparing their binding energy to the graphitic materials with the binding energy of the corresponding crystals. This amounts to computing the binding energy of the metal atoms inserted in graphite *taking the result for the crystalline metal as the reference of energy*. For example, the binding energy of Be in C_6Be would be: $E(\text{Be crystal}) + E(\text{graphite}) - E(C_6Be)$, where $E(\text{Be crystal})$ is the energy per atom of the Be crystal, etc. A positive value of a binding energy thus computed would be a strong indication that the metal atoms will *not* segregate to form clusters. Note that, since the cohesive energy per atom is larger for the crystal than for a cluster, the proposed criterion will tend to overestimate the tendency to segregate. (Typically, the energy of the isolated metal atom should be used as a reference for the computation of the binding energy; note that binding energies thus obtained – e.g., those reported in Ref. 35, which discusses the role of long-range forces in this type of systems – cannot be compared with ours directly.)

An important difficulty with the application of the above criterion relates to the disparity of the forces that dominate the binding in each of the the systems whose energies are to be compared. Indeed, while both the LDA and GGA can be expected to be accurate for the metallic crystals, only the LDA looks like a reasonable option for graphite, and the GGA should be the more accurate for the metal-intercalated materials. Being aware of these difficulties, we have performed both LDA and GGA calculations, which allows us to have some confidence in the trends observed. (For the GGA calculation of $E(\text{graphite})$, we used the lowest-energy structure obtained from our LDA calculation, as the GGA-relaxed structure deviates significantly from the experimental one.)

Table III thus reports our results for the binding energies of metal atoms to the C_6M systems and, for the sake of comparison, to an isolated graphene layer. The main conclusion is that, as expected, the metal atoms inserted in the graphitic structures can be expected to be substantially more resistant to clustering than those deposited on graphene. Indeed, for many elements, like the considered alkali metals and Ca, our prediction is that the metal

TABLE III: Calculated binding energies (in eV) of metal atoms to an isolated graphene layer (the simulated Gr.-M systems correspond to the $C_{32}M$ formula unit) and graphite (corresponding to the composition C_6M). Both LDA and GGA results are given. (See text for more details.)

		LDA binding energies					
		Li	Na	K	Be	Mg	Ca
Gr.-M		-0.40	-0.56	-0.16	-3.91	-1.62	-1.54
C_6M		0.60	0.20	0.70	-1.98	-1.15	0.16
		Sc	Ti	V	Y	Zr	
Gr.-M		-2.75	-3.89	-4.76	-2.67	-4.44	
C_6M		0.52	-0.46	-1.40	0.58	-0.43	
		GGA binding energies					
		Li	Na	K	Be	Mg	Ca
Gr.-M		-0.76	-0.85	-0.18	-3.70	-1.48	-1.54
C_6M		0.38	0.15	0.44	-2.27	-1.28	0.46
		Sc	Ti	V	Y	Zr	
Gr.-M		-2.97	-3.83	-4.40	-2.92	-4.42	
C_6M		-0.03	-1.30	-1.92	-0.22	-0.93	

atoms will not segregate at all. This result is compatible with the experimental fact that there exist low-stage metal-intercalated carbons for Li, K, and Ca. In what regards the alkaline earth species that are most promising for hydrogen-storage purposes, i.e. Be and Mg, the calculations suggest they might present a tendency towards segregation even in the intercalated graphitic materials. The causes for the computed, relatively weak, binding of Be and Mg to the carbon structure are probably related with (i) the stable closed-shell electronic structure of these atoms and (ii) their preference for coordinations that are lower than those typical of the alkali and Ca metals (note that Be and Mg crystallize in an hexagonal structure in which atoms are less coordinated than in the cubic alkali and Ca metals). As for the transition metals, the calculations also suggest a tendency to segregate, although not as strong as for Be and Mg. Finally, let us note that in a few cases we computed the binding energies for different C-M ratios; the observed variations, of up to a few tenths of eV when moving from C_4M to $C_{14}M$, are not significant given the approximations involved in our estimates.

In conclusion, our results indicate that Be and Mg, the most promising elements from the hydrogen-storage perspective, are also the most likely ones to undergo segregation and cluster formation when intercalated in graphitic structures. Nevertheless, given the crudeness of the approximations made, we think this result should not discourage experimental attempts at verifying the hydrogen-storage mechanism predicted to occur in the Be- and Mg-intercalated materials.

IV. SUMMARY AND CONCLUSIONS

In summary, we have studied the hydrogen-binding properties of various stage-one metal-intercalated graphites, which are idealized model systems that we assume capture the relevant metal-hydrogen interactions that would be present in other, structurally more complex, graphitic materials.

In agreement with the experimental literature, we find that alkali metals induce an expansion of the graphene-graphene interlayer distance which, in turn, facilitates the hydrogen absorption. Hydrogen is absorbed in molecular form and weakly bound to the carbon structure, which results in a relatively large effective size and, consequently, a low storage capacity. We have also studied a number of transition metal atoms (namely, light *3d* and *4d* elements) and obtained discouraging results in what regards hydrogen storage: our simulations predict relatively strong carbon-metal interactions that result in narrow interlayer spaces and prevent the metal atoms from acting as convenient binding sites for hydrogen.

Remarkably, we obtain very promising results for the alkaline earth metals. For all the elements studied (namely, Be, Mg, and Ca), we observe that the intercalated metal atoms interact strongly with the H₂ molecules and form metal-hydrogen complexes. Our results indicate that each metal atom can bind a maximum of three or four hydrogen molecules, the binding energies ranging from 0.2 to 0.7 eV, as required for hydrogen-

storage applications. The storage capacity, predicted for the simulated stage-one graphites intercalated with Be and Mg, can reach values in the 7-8 wt% range.

In conclusion, our simulations indicate that alkaline earth metals are the best option to try to obtain graphitic materials with an enhanced hydrogen-storage performance. Some of our predictions could be directly tested by measuring the hydrogen-absorption properties of the recently obtained stage-one intercalated graphite C₆Ca.⁸ Yet, it must be stressed that the theory suggests that Be and Mg based compounds may offer a superior performance. We hope that the novel possibilities discussed in this paper will aid current, and encourage new, experimental efforts aimed at producing a competitive carbon-based hydrogen-storage system.

We acknowledge useful discussions with C. Ahn, E. Canadell, M.H. Cohen, C. Contescu, K.S. Nahm, G. Walker, and T. Yildirim. This is work made in the context of our participation in Task 22 of the International Energy Agency's Hydrogen Implementing Agreement. It was financially supported by the Spanish Ministry of Science and Education (ENE2006-27257-E, FIS2006-12117-C04-01 and CSD2007-00041) and the Catalan Government (SGR2005-683).

References

-
- ¹ M. Hirscher and M. Becher, *J. Nanoscience and Nanotechnology* **3**, 3 (2003).
 - ² T. Yildirim and S. Ciraci, *Phys. Rev. Lett.* **94**, 175501 (2005).
 - ³ Y. Zhao, Y.-H. Kim, A.C. Dillon, M.J. Heben, and S.B. Zhang, *Phys. Rev. Lett.* **94**, 155504 (2005).
 - ⁴ T. Yildirim, J. Íñiguez, and S. Ciraci, *Phys. Rev. B* **72**, 153403 (2005).
 - ⁵ Q. Sun, P. Jena, Q. Wang, and M. Marquez, *J. Am. Chem. Soc.* **128**, 9741 (2006).
 - ⁶ H.-S. Kim *et al.*, *J. Phys. Chem. B* **109**, 8983 (2005).
 - ⁷ J.W. Lee, H.S. Kim, J.Y. Lee, and J.K. Kang, *Appl. Phys. Lett.* **88**, 143126 (2006).
 - ⁸ N. Emery *et al.*, *Phys. Rev. Lett.* **95**, 087003 (2005).
 - ⁹ N. Emery, C. Hérold, and P. Lagrange, *J. Sol. St. Chem.* **178**, 2947 (2005).
 - ¹⁰ M.S. Dresselhaus and G. Dresselhaus, *Adv. Phys.* **30**, 139 (1981).
 - ¹¹ P. Hohenberg and W. Kohn, *Phys. Rev.* **136**, B864 (1964).
 - ¹² W. Kohn and L.J. Sham, *Phys. Rev.* **140**, A1133 (1965).
 - ¹³ G. Kresse and J. Furthmüller, *Phys. Rev. B* **54**, 11169 (1996).
 - ¹⁴ J.P. Perdew and A. Zunger, *Phys. Rev. B* **23**, 5048 (1981).
 - ¹⁵ D.M. Ceperley and B.J. Alder, *Phys. Rev. Lett.* **45**, 566 (1980).
 - ¹⁶ J.P. Perdew, K. Burke, and M. Ernzerhof, *Phys. Rev. Lett.* **77**, 3865 (1996).
 - ¹⁷ P. E. Blochl, *Phys. Rev. B* **50**, 17953 (1994).
 - ¹⁸ G. Kresse and D. Joubert, *Phys. Rev. B* **59**, 1758 (1999).
 - ¹⁹ S. Baroni, A. Dal Corso, S. de Gironcoli, and P. Giannozzi, <http://www.pwscf.org/>.
 - ²⁰ J.S. Arellano, L.M. Molina, A. Rubio, and J.A. Alonso, *J. Chem. Phys.* **112**, 8114 (2000).
 - ²¹ K. Tada, S. Furuya, and K. Watanabe, *Phys. Rev. B* **63**, 155405 (2001).
 - ²² D. Henwood and J.D. Carey, *Phys. Rev. B* **75**, 245413 (2007).
 - ²³ A. Ferre-Vilaplana, *J. Chem. Phys.* **122**, 104709 (2005).
 - ²⁴ P.O. Löwdin, *J. Chem. Phys.* **18**, 365 (1950).
 - ²⁵ N. Jacobson, B. Tegner, E. Schröder, P. Hyldgaard, and B.I. Lundqvist, *Comp. Mats. Sci.* **24**, 273 (2002).
 - ²⁶ K. Watanabe, T. Kondow, M. Soma, T. Onishi, and K. Tamaru, *Proc. R. Soc. London A* **333**, 51 (1973).
 - ²⁷ I. Cabria, M.J. López, and J.A. Alonso, *J. Chem. Phys.* **123**, 204721 (2005).
 - ²⁸ R.C. Lochan and M. Head-Gordon, *Phys. Chem. Chem. Phys.* **8**, 1357 (2006).
 - ²⁹ H. Cheng, G. Pez, G. Kern, G. Kresse, and J. Hafner, *J. Phys. Chem.* **105**, 736 (2001).
 - ³⁰ K. Watanabe, M. Soma, T. Onishi, and K. Tamaru, *Nature Physical Sci.* **233**, 160 (1971).
 - ³¹ P. Lagrange, A. Métrot, and A. Hérold, *C.R. Acad. Sc. Paris* **275**, 765 (1972).
 - ³² K.N. Semenenko, S.N. Klyamkin, V.A. Nalimova, and A.A.

Karikh, *Carbon* **32**, 1025 (1994).

³³ The figures of wave functions were generated using the visualization software described in A. Kokalj, *J. Mol. Graphics Modelling* **17**, 176 (1999); <http://www.xcrysden.org/>.

³⁴ G.J. Kubas, *Metal Dihydrogen and Bond Complexes*

– *Structure, Theory, and Reactivity* (Kluwer Academic/Plenum, Dordrecht, 2001).

³⁵ A. Lugo-Solis and I. Vasilev, *Phys. Rev. B* **76**, 235431 (2007).